

FROM BILLIARDS TO THERMODYNAMIC LAWS: STOCHASTIC ENERGY EXCHANGE MODEL

YAO LI

Yao Li: Department of Mathematics and Statistics, University of Massachusetts Amherst, Amherst, MA, 01002, USA

LINGCHEN BU

Lingchen Bu: Department of Mathematics and Statistics, University of Massachusetts Amherst, Amherst, MA, 01002, USA

ABSTRACT. This paper studies a billiards-like microscopic heat conduction model, which describes the dynamics of gas molecules in a long tube with thermalized boundary. We numerically investigate the law of energy exchange between adjacent cells. A stochastic energy exchange model that preserves these properties is then derived. We further numerically justified that the stochastic energy exchange model preserves the ergodicity and the thermal conductivity of the original billiard model.

The derivation of macroscopic thermodynamic laws from microscopic Hamiltonian dynamics is a century-old challenge dating back to Boltzmann. In this paper, we use a billiards-like Hamiltonian model to study the microscopic heat conduction of gas molecules in a long tube. After a series of numerical simulation, a mathematically tractable stochastic energy exchange model is derived. We further show that many key properties of the original deterministic problem are preserved by this stochastic energy exchange model. This result opens the door to rigorous justifications of many interesting problems in nonequilibrium statistical mechanics. In our forthcoming papers, we will study the ergodicity, mesoscopic limit, and macroscopic thermodynamic laws of the stochastic energy exchange model derived in this paper.

1. INTRODUCTION

in a nonequilibrium setting, it is very difficult to prove that deterministic interactions among gas molecules or crystal structures leads to macroscopic thermodynamic laws such as Fourier's law [2]. From a dynamical systems point of view, deterministic interactions of gas molecules can be modeled as elastic collisions of particles.

E-mail addresses: yaoli@math.umass.edu, lingchen.l.bu@gmail.com.

However, studying many-particle billiard systems is a very difficult, with only limited known result [4, 47, 48]. It is almost impossible to provide any mathematical derivation of macroscopic thermodynamic laws by working on a many-particle billiard model. Most known results that connect dynamical billiards and thermodynamics are for one particle model, noninteracting particles, and weakly interacting particles [13, 1, 32, 11, 10].

On the other hand, there are also many stochastic microscopic heat conduction models which assume some randomness among particle interactions or energy transports. Stochastic interacting particle models are known to be more tractable. There have been numerous known results about nonequilibrium steady-state, entropy production rate, fluctuation theorem, thermal conductivity, and Fourier’s law for various stochastic models [15, 20, 27, 40, 12, 14, 44, 45]. Therefore, it is tempting to reduce a deterministic heat conduction model to a stochastic one. One example is [38], in which a particle-disk collision model is well-approximated by a stochastic particle system.

This paper serves as the first paper of a sequel. In this sequel, we will investigate how thermodynamic laws are derived from billiards-like deterministic dynamics. Different from many pioneering work, the billiard system in our study consists of a large number of strongly interacting particles, which makes a rigorous study extremely difficult. The goal of this paper is to numerically justify that the deterministic dynamics in a billiards-like dynamical system is well-approximated by a Markovian energy exchange process. We carry out a series of numerical simulations to determine the rule of stochastic energy exchanges. Then we will use computer-assisted method proposed in [36] to justify that the resultant stochastic energy exchange model preserves many key properties of the original deterministic dynamics, such as ergodicity and thermal conductivity.

Consider many gas particles in a long and thin tube as in Figure 1 (top). Assume further that two ends of the tube is connected to heat baths with different temperatures. For the sake of simplicity, we assume gas particles only do free motion and elastic collisions. When a particle hits the left (or right) boundary, a random particle drawn from a Boltzmann distribution is chosen to collide with this particle. Besides that, everything else is purely deterministic. Needless to say, any analysis of such a strongly interacting multi-body problem is extremely difficult. On the other hand, usually a gas particle collides with other particles very frequently. At ambient pressure, the mean free path of a gas molecule is as short as 68 nm [24]. Therefore, motivated by earlier studies [3, 17, 16, 18], we propose to simplify the model by localizing gas molecules in a chain of cells as in Figure 1 (bottom). Disk-shaped particles are assumed to be trapped in those 2D cells, each of which is a chaotic billiard table. Adjacent cells are connected by a “gate”. Particles can not pass the “gate” but can collide through it. This gives the *nonequilibrium billiard model* introduced in Section 2. Throughout this paper, we assume that each cell contains M particles. M is a fixed finite number.

Since the motion of gas particles is highly chaotic, a particle has quick loss of memory. In fact, it is known that a chaotic billiard system usually have good

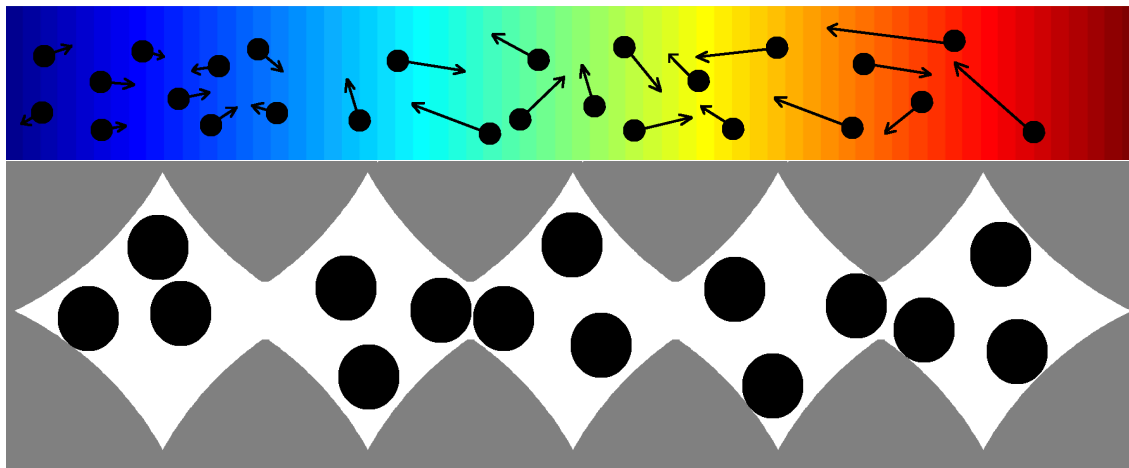


FIGURE 1. Top: Gas molecules in a tube. Bottom: Particles are trapped in a chain of cells. Particles can collide through the “gate”.

statistical properties [5, 6, 8, 9]. That is why we believe a Markov model should well approximate such a billiard model. In order to make the billiard model mathematics tractable, instead of modeling each particle, we choose to look for a Markov process that describes the time evolution of the total energy stored in each cell. When particles in neighbor cells collide, we let the corresponding cells exchange a certain random amount of energy. This Markov process is called the *stochastic energy exchange model*. Due to the significant difficulty of studying a multibody billiard system, a rigorous derivation of this Markov process is not possible. Instead, we use numerical simulation to justify this model reduction.

One needs to answer two questions in order to find the rule of stochastic energy exchange model: *when* and *how* two particles in neighbor cells exchange energy. To answer these questions, a series of numerical studies are carried out in Section 3. We find that the time distribution to the next collision between particles from adjacent cells is not visually distinguishable from an exponential distribution. Therefore, one exponential clock should be associated with each adjacent pair of cells. The rate of this exponential clock is approximately square root of the minimum of two energies at the tail, as a low total energy in a cell is always associated with a long time interval between two energy exchanges. The rule of energy exchange is more complicated. But after some numerical simulations, we find a simple rule that can preserve qualitative properties that we are interested in. The energy of the particle that participates the collision satisfies a Beta distribution. After the collision, the energy is uniformly redistributed. Although this is not exactly a precise rule of energy distribution at a collision, it is simple enough while preserves the tail distribution on the low energy side, which determines asymptotic properties of the system. Although the entire reduction to a Markov process is not rigorous, we attempt to provide as much mathematical justification as possible based on several assumptions that heuristically should be valid for sufficiently chaotic interacting particle system.

The stochastic energy exchange model is then summarized in the end of Section 3. Then we compared those two models from the aspects of ergodicity and thermal conductivity. In Section 4, we numerically show that both models has polynomial ergodicity $\sim t^{-2M}$, where M is the number of particles in each cell. Due to the significant difficult of direct simulations, for the billiard model, we use Monte Carlo simulation to compute the first passage time to a “high-energy state”, same as done in [33]. For the stochastic energy exchange model, we adopt a computer assisted method proposed in [36]. Some key estimations regarding return times are obtained numerically, while other ingredients are rigorous. We show that the stochastic energy exchange process admits a unique nonequilibrium steady state. The speed of convergence to this steady state, and the speed of correlation decay, are both polynomial. Finally, in Section 5, we compute the thermal conductivity of the stochastic energy exchange model. We find that the thermal conductivity is proportional to $1/N$, which is consistent with early study of the billiard model in [17, 16] (with one particle in each cell).

2. NONEQUILIBRIUM BILLIARD MODEL FOR MICROSCOPIC HEAT CONDUCTION

As discussed in the introduction, it is difficult to study the dynamics when a large number of gas molecules moving and interacting in a tube. Since the mean free path of a gas molecule is very short, we “localize” gas molecules into a chain of cells to simplify the dynamics. The precise description of this locally confined particle system is as follows.

Consider an 1D chain of N connected billiard tables in \mathbb{R}^2 , denoted by $\Omega_1, \dots, \Omega_N$. Each table is a subset of \mathbb{R}^2 whose boundary is formed by finitely many piecewise C^3 curves. Neighboring billiard tables are connected by one or finitely many “bottleneck” openings. The first and the last tables are connected to the heat bath. The interaction with the heat bath will be described later.

Let M be a positive integer that is fixed throughout this section. Assume inside each billiard table there are M rigid moving disks with mass 2 and radius r . Each disk-shaped particle moves freely until it hits the boundary of the billiard table, or other particles. The configuration of a state of particles in the n -th cell is denoted by $(\mathbf{x}_1^n, \mathbf{v}_1^n, \dots, \mathbf{x}_M^n, \mathbf{v}_M^n)$, where $\mathbf{x}_k^n \in \mathbb{R}^2$ and $\mathbf{v}_k^n \in \mathbb{R}^2$ are position (of the center) and velocity of the k -th particle in the n -th cell respectively. We assume the following for this billiard system.

- A particle is trapped in the cell in a way that its trajectory will never leave Ω_n .
- Particles in neighbor cells can collide with each other without passing through the opening between cells.
- All collisions are elastic. Particles do not rotate.
- The billiard system is chaotic.
- Let $\Gamma_n \subset \Omega_n$ be the collection of possible positions of particles in the n -th table. There exist positions $\mathbf{x}_1^n, \dots, \mathbf{x}_M^n$ and $\epsilon > 0$ such that

$$|\mathbf{x}_i^n - \mathbf{x}_j^n| > 2r + \epsilon \text{ for all } i, j = 1 \sim M, i \neq j$$

and

$$\bigcup_{i=1}^M B(\mathbf{x}_i^n, R + \epsilon) \subset \Gamma_n \setminus \bigcup_{|m-n|=1} B(\Gamma_m, r).$$

In other words particles in a table can be completely out of reach by their neighbors. In addition a cell is sufficiently large such that particles won't get stuck.

Now we couple this chain with two heat baths. The temperature of two heat baths are T_L and T_R respectively. We assume that the heat bath is a billiard table with the same geometry and the same number of moving particles. But the total energy in the heat bath is randomly chosen. The rule of the heat bath interaction is the following. At the beginning a random total energy E_L (resp. E_R) is chosen for the left (resp. right) heat bath from the exponential distribution with mean T_L (resp. T_R). The initial distribution of particle positions and velocities satisfies the conditional Liouville measure (conditioning with the total energy E_L). This system is evolved deterministically until the first collision between a heat bath particle and a “regular” particle in the leftmost (resp. rightmost) table. Immediately after such a collision, particles in the heat bath are independently redistributed with a new total energy and new initial positions/velocities, which are drawn from the same distribution. This is an idealized way to approximate the interaction with a heat bath that has infinitely many particles.

Let

$$\Omega = \{(\mathbf{x}_1^1, \mathbf{v}_1^1, \dots, \mathbf{x}_M^1, \mathbf{v}_M^1), \dots, (\mathbf{x}_1^N, \mathbf{v}_1^N, \dots, \mathbf{x}_M^N, \mathbf{v}_M^N)\} \subset \mathbb{R}^{4MN}$$

be the state space of this billiard model. Let $\Phi_t : \Omega \rightarrow \Omega$ be the flow generated by the billiard model. It is easy to see that Φ_t is a piecewise deterministic Markov process.

3. REDUCTION TO STOCHASTIC ENERGY EXCHANGE MODEL

In order to make the nonequilibrium billiard model introduced in Section 2 tractable for further rigorous studies, we need to consider the evolution of some coarse-grained variables instead of velocities and positions of all particles. As introduced in the introduction, we look for a Markov process that describes the time evolution of total energy stored in each cell.

The aim of this section is to provide numerical and mathematical justifications of such reduction from the deterministic billiard model to a stochastic energy exchange model. We remark that this section is *not* intended to be mathematically rigorous. In fact, any rigorous study of a billiard system with more than one moving particle is extremely difficult, with fairly limited known results [28, 46, 48, 47]. Therefore, mathematical justifications in this section have to be built on various heuristic assumptions. We provide as much mathematical justifications as possible for each argument we raise. The conclusion is then verified by carefully designed numerical simulations.

In the following two subsections, we study *when* and *how* an energy exchange between two adjacent cells, i.e., a collision between two particles from each cell

respectively, should happen. The setting of our numerical simulation is as follows. The boundary of two cells is determined by 6 circles and 2 line segments as seen in Figure 2. In each cell, there are M particles undergoing free motion and elastic collisions. We use Monte Carlo simulation to study the distribution of collision times and the distribution of energy transferred during a collision.

Cells in Figure 2 are designed such that all cell boundaries are either flat or convex inwards, which makes motion of all particles chaotic [7]. Recall that our main requirement of the cell geometry is that it should generate a chaotic billiard system. We expect our numerical result to be valid for any nonequilibrium billiard model that satisfies our assumptions.

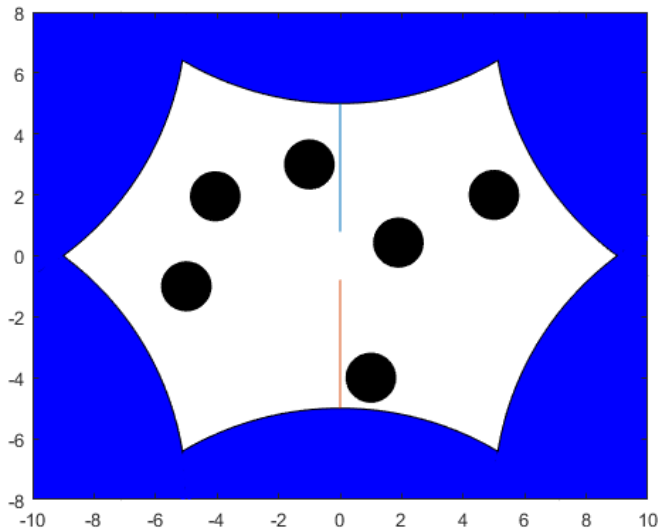


FIGURE 2. Setting of our numerical simulations. Two adjacent cells with three particles in each cell. Particles can collide through the gate, but can't pass through the gate.

3.1. Distribution of collision time. The first numerical result is about the time distribution of energy exchanges between particles from neighboring cells, called the *collision time*. The deterministic billiard model is highly chaotic, which heuristically indicates a quick decay of correlation. This is the main motivation for us to look for its Markovian approximation. Due to the quick correlation decay, we expect collision times between particles from adjacent cells to be close to an inhomogeneous Poisson process. This is to say, when starting from a fixed energy configuration, the first collision time should be well-approximated by an exponential distribution. Further, conditioning on the same energy configuration, the time duration between two consecutive collisions should also satisfy an exponential distribution with the same rate. In dynamical systems, these two distributions are called the *hitting time* and the *return time* respectively. It is known that for a strongly mixing dynamical system, those two times to an asymptotically small set coincides [22, 23]. We provide

the following simulations to study distributions of the hitting time and the return time of the billiard model.

Rate of hitting time. Define the random variable

$$(3.1) \quad \tau_c = \inf\{t > 0 \mid \text{a cell-cell collision occurs at time } t\}.$$

If the collision time is Poisson distributed, we should have

$$(3.2) \quad P(\tau_c > t) = \int_t^{+\infty} \lambda e^{-\lambda x} dx = e^{-\lambda t}.$$

In other words the rate of this Poisson distribution is $\lambda = -\frac{1}{t} \log P(\tau_c > t)$. However, the collision time is not Poisson distributed because the energy process produced by the billiard model is clearly not Markovian. Instead, we expect the distribution of τ_c to have an exponential tail. The slope of such tail, if exists, is called the stochastic energy exchange rate. More precisely, we are interested in $\lim_{t \rightarrow \infty} -\frac{1}{t} \log P(\tau_c > t)$.

Consider an energy configuration (E_1, E_2) that corresponds to total cell energy E_1 and E_2 in the left cell and right cell respectively. Let π be the Liouville measure with respect to two cells and their $2M$ particles, which is an invariant measure of the billiard system involving two neighboring cells. A function $R(E_1, E_2)$ is said to be a *stochastic energy exchange rate* if

$$(3.3)$$

$$(3.4) \quad \begin{aligned} R(E_1, E_2) &= \lim_{t \rightarrow \infty} -\frac{1}{t} \log P_\pi[\tau_c > t \mid \sum_{i=1}^M |\mathbf{v}_i^1|^2 = E_1, \sum_{i=1}^M |\mathbf{v}_i^2|^2 = E_2] \\ &= \lim_{t \rightarrow \infty} -\frac{1}{t} \log P_\pi[\tau_c > t \mid \sum_{i=1}^M |\mathbf{v}_i^1(0^+)|^2 = E_1, \sum_{i=1}^M |\mathbf{v}_i(0^+)|^2 = E_2], \end{aligned}$$

$$(3.5) \quad \mathbf{x}_i^1 \in \text{int}(\Gamma_1), \mathbf{x}_j^2 \in \text{int}(\Gamma_2), |\mathbf{x}_i^1(0^+) - \mathbf{x}_j^2(0^+)| = 2r \text{ for some } 1 \leq i, j \leq M$$

is well-defined. The first limit gives the tail of the first collision time distribution when starting from a conditioning Liouville measure (conditioning with the energy configuration (E_1, E_2)). The second limit gives the tail of return time distribution, when starting from the configuration corresponding to an energy exchange event.

Note that obviously $R(\alpha E_1, \alpha E_2) = \alpha^{1/2} R(E_1, E_2)$, we only need to simulate the case of $E_1 + E_2 = 1$. Without loss of generality we assume $E_1 \leq E_2$. We use Monte Carlo simulations to compute distributions of τ_c for $M = 2, 3, 4$. For each M , we use 26 different initial energy configurations $E_1 = 0.5, 0.4, 0.3, 0.2, 0.1, 0.05, 0.02, 0.01, 5 \times 10^{-3}, 2 \times 10^{-3}, 1 \times 10^{-3}, 5 \times 10^{-4}, 2 \times 10^{-4}, 1 \times 10^{-4}, 5 \times 10^{-5}, 2 \times 10^{-5}, 1 \times 10^{-5}, 5 \times 10^{-6}, 2 \times 10^{-6}, 1 \times 10^{-6}, 5 \times 10^{-7}, 2 \times 10^{-7}, 1 \times 10^{-7}, 5 \times 10^{-8}, 2 \times 10^{-8}, 1 \times 10^{-8}$. The initial distribution is a conditional Liouville measure, at which the initial particle positions are uniformly distributed, and the initial particle velocities are uniformly distributed on a sub-manifold of \mathbb{S}^{4M} such that $|\mathbf{v}_i^1(0^+)|^2 = E_1, \sum_{i=1}^M |\mathbf{v}_i(0^+)|^2 = E_2$. The energy exchange rate $R(E_1, E_2)$ is obtained by calculating the slope of distributions of τ_c in log-linear plots.

Figure 3 shows three sample distribution curves of τ_c starting from different energy configurations. The probability $\mathbb{P}[\tau_c > t]$ forms a straight line in the log-linear plot

until there are not enough samples with $\tau_c > t$. In fact, for all energy configurations we have tested, one can not visually distinguish the distribution of τ_c from that of a genuine exponential distribution. This numerically verifies our assumption that the distribution of τ_c always has an exponential tail.

Then we present the result $R(E_1, E_2)$ versus E_1 for $M = 2, 3, 4$, which is plotted in Figure 4. This is consistent with our numerical finding in [33]. We are more interested in the scaling of R as $E_1 \rightarrow 0$. From the slope in the log-log plot in Figure 4, we can see that $R(E_1, E_2) \sim \sqrt{\min\{E_1, E_2\}}$ when $\min\{E_1, E_2\} \ll 1$ in all three cases.

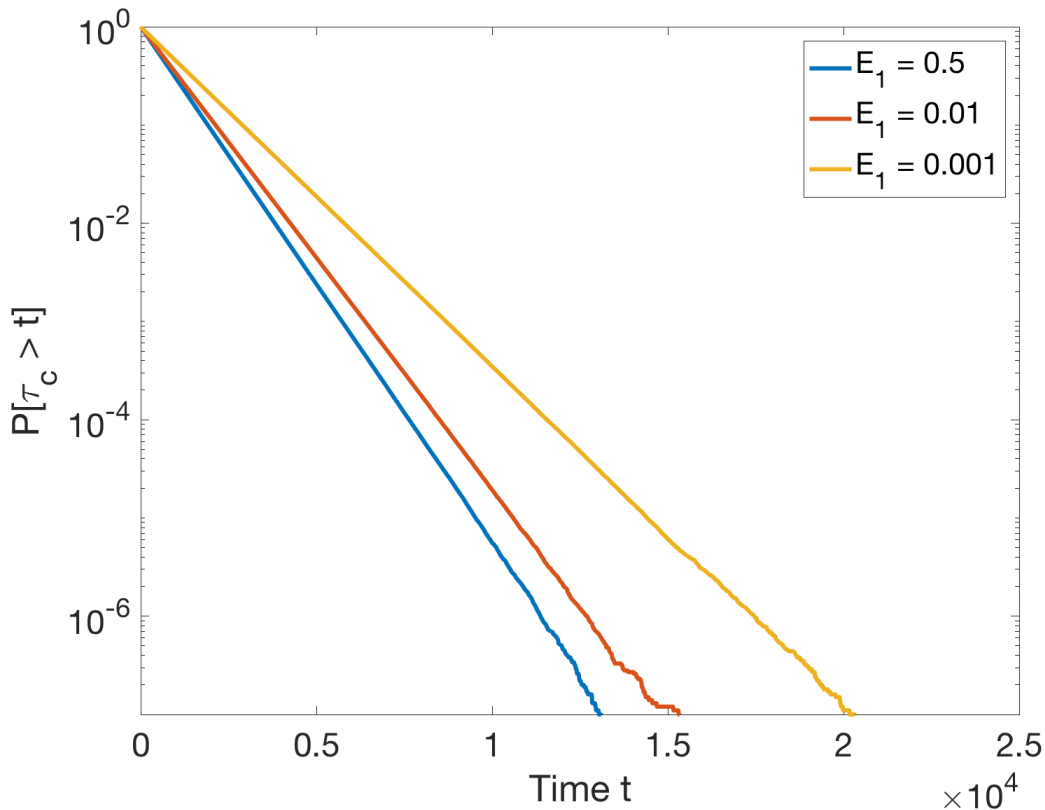


FIGURE 3. Three examples of distributions of τ_c with $E_1 = 0.5, 0.01$ and 0.001 . Each cell has 3 moving particles. Each distribution is obtained by running 10^8 independent trajectories until the first collision time.

Hitting time vs. return time. It remains to verify that the second limit in (3.3) produces the same tail. This is to say, we need to check that when conditioning on the same energy configuration, the distribution of time duration between two consecutive collision times, called the *conditional return time*, has the same exponential tail. Let $(E_1^{(1)}, E_2^{(1)}, t^{(1)}), (E_1^{(2)}, E_2^{(2)}, t^{(1)} + t^{(2)}), \dots, (E_1^{(N)}, E_2^{(N)}, t^{(1)} + \dots + t^{(N)})$ be a long trajectory sampled at collision times from a simulation starting from \mathbf{x}_0 . Same as in [33], we expect to have a joint probability density function $\rho_{\mathbf{x}_0}(E_1, E_2, t)$ about

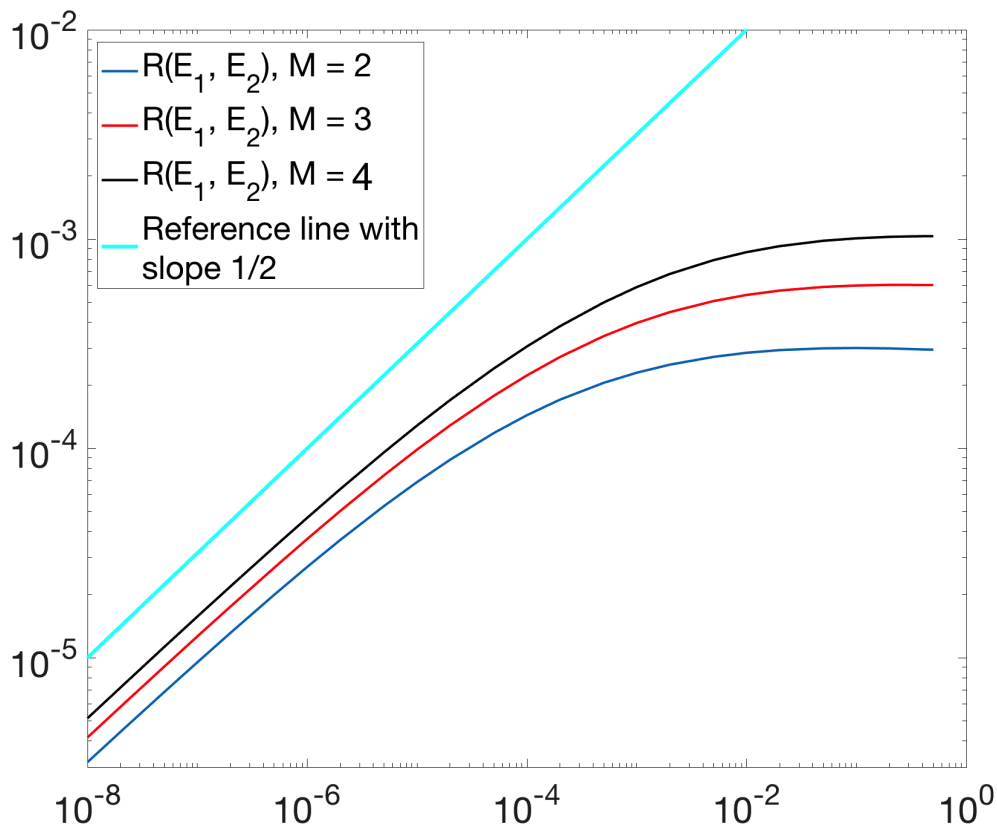


FIGURE 4. $R(E_1, E_2)$ versus E_1 in log-log plot for $M = 2, 3, 4$ with constraint $E_1 + E_2 = 1$. The initial distribution is a conditional Liouville measure conditioning on the energy configuration (E_1, E_2) . For each M , 26 different initial energy configurations (E_1, E_2) with are chosen. The distribution of τ_c is obtained by running 10^8 trajectories until the first collision time. For each energy configuration, $R(E_1, E_2)$ is the slope of τ_c in the log-linear plot.

the conditional return time and the energy configuration. Further, if $R(E_1, E_2)$ is well-defined, we should have

$$(3.6) \quad \lim_{t \rightarrow \infty} \frac{1}{t} \log \left(\int_t^\infty \rho_{\mathbf{x}_0}(E_1, E_2, s) |_{(E_1, E_2)} ds \right) = R(E_1, E_2).$$

Assume $E_1 + E_2 = 1$. We define the following rescaled return time

$$(3.7) \quad \Lambda(t) = \int_t^\infty \rho_{x_0}(E, 1 - E, s) R(E, 1 - E) dE ds.$$

If the exponential tail of $\rho_{\mathbf{x}_0}(E_1, E_2, s) |_{(E_1, E_2)}$ has the same slope $R(E_1, E_2)$ in a log-linear plot, $\Lambda(t)$ should have a tail e^{-t} . It is easy to see that $\Lambda(t)$ can be sampled by $\{t^i R(E_1^{(i)}, E_2^{(i)})\}$, where $R(E_1, E_2)$ is obtained from Figure 5. The estimator of

$\Lambda(t)$ is

$$(3.8) \quad \hat{\Lambda}(t) = \frac{1}{N} \left| \{t^i R(E_1^{(i)}, E_2^{(i)}) > t\} \right|,$$

where N is the sample size of the Monte Carlo simulation.

In Figure 5, we can see that $\hat{\Lambda}(t)$ matches e^{-t} very well for $M = 2, 3, 4$. This verifies that the conditional return time coincides with the first collision time.

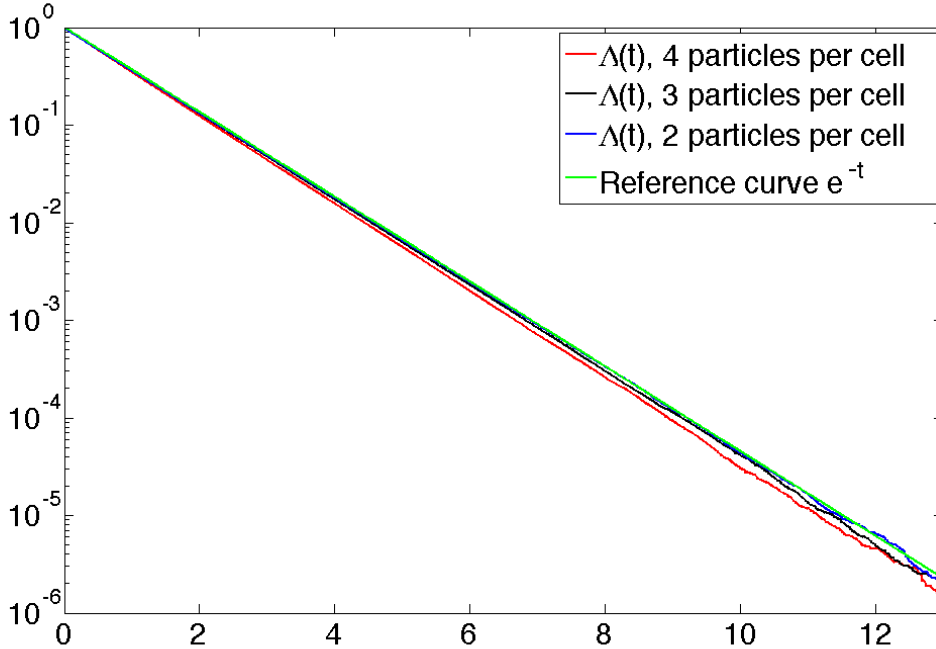


FIGURE 5. $\hat{\Lambda}(t)$ from long trajectories for $M = 2, 3, 4$. $\hat{\Lambda}(t)$ is obtained from equation (3.8). Sample size of each simulation is $N = 10^8$.

3.2. Rule of energy exchange. The second study aims to reveal the rule of energy exchange at a collision. We separate this problem into two parts:

- (a) The energy distribution of a particle that participates in a collision.
- (b) The rule of the energy redistribution during the collision.

If there is only one particle in a cell, (a) becomes trivial. Otherwise, consider M particles collide with each other in a chaotic billiard table. Due to the quick correlation decay, this billiard system should converge to its invariant measure, i.e., the Liouville measure, in a short time. At the Liouville measure, the velocity distribution of these M particles is a uniform distribution on a $(2M - 1)$ -sphere. Assume particle velocities are uniformly distributed on a $(2M - 1)$ -sphere, some easy calculation in Proposition 3.1 shows that the energy distribution of a particle is a Beta distribution with parameters $(1, M - 1)$.

Proposition 3.1. *Let (X_1, \dots, X_{2M}) be a uniform distribution on the surface \mathbb{S}^{2M-1} . Then $X_1^2 + X_2^2$ has Beta distribution with parameters $(1, M - 1)$.*

Proof. Let Y_1, \dots, Y_{2M} be $2M$ standard normal random variables. Let

$$(3.9) \quad X_i = \frac{Y_i}{\sqrt{Y_1^2 + \dots + Y_{2M}^2}}.$$

Then it is well known that (X_1, \dots, X_{2M}) gives a uniform distribution on the surface of a unit $(2M - 1)$ -sphere. Therefore, we have

$$(3.10) \quad X_1^2 + X_2^2 = \frac{Y_1^2 + Y_2^2}{\sum_{i=1}^{2M} Y_i^2} := \frac{\Gamma_1}{\Gamma_1 + \Gamma_2},$$

where Γ_1 is a $\Gamma(1, 2)$ distribution and Γ_2 is a $\Gamma(M - 1, 2)$ distribution. The ratio $\Gamma_1/(\Gamma_1 + \Gamma_2)$ is a Beta distribution with parameters $(1, M - 1)$. \square

Since each cell in the nonequilibrium billiard model forms a chaotic billiard table, it is reasonable to assume that at the collision time, the M -particle system in a cell is close to its invariant measure. Hence the energy distribution of any given particle is approximated by a Beta distribution with parameters $(1, M - 1)$.

Some corrections need to be added to the Beta distribution to approximate the energy distribution of the particle that *participates in* a collision between particles from neighboring cells. The reason is that faster particles have higher chance to participate in such a collision. Hence the distribution should be biased towards high energy states. This bias can be estimated by the following heuristic arguments.

The billiard system in each cell is assumed to be sufficiently chaotic, which means the correlation decays quickly. Hence it is reasonable to assume that at the collision time, particle energies in neighboring cells are independent. Consider a pair of consecutive cells with an energy configuration (E_1, E_2) . Let x_L and x_R be the ratio of the energy of the colliding particle to the total energy of its cell. Because of the independence assumption, the probability density of x_L should be proportional to $A(t)$, where t is the “effective time” that a particle from the right table is available for a collision, and $A(t)$ is the area swiped by a particle during the time $(0, t)$.

We only study the energy distribution of the left particle, as the right one follows from an analogous argument. It is obvious that

$$(3.11) \quad A(t) = \pi R^2 + 2R|v|t,$$

where $|v| = \sqrt{E_1 x_L}$. It is not easy to give an explicit expression of the “effective time”, but heuristically t should be proportional to

$$(3.12) \quad \frac{R}{\sqrt{E_2}} \cdot \frac{\sqrt{E_1}}{\sqrt{E_2}},$$

where the first term approximates the time duration that a particle from the right stays at the gate area, and the second term is the ratio of “time scales” in two cells. Hence we have

$$(3.13) \quad A(t) = \pi R^2 + 2CR^2 \frac{E_1}{E_2} \sqrt{x_L},$$

where C is a constant that depends on the geometry of the model. Combine with Proposition 3.1, we conclude that the probability density of x_L should be approximated by

$$(3.14) \quad w(x_L) = \frac{1}{K} \left(1 + C \frac{E_1}{E_2} \sqrt{x_L}\right) (1 - x_L)^{M-2}$$

if $M \geq 2$, where K is a normalizer.

This heuristic argument is verified by our numerical results. In Figure 6, we compare the approximation (3.14) with simulation results of x_L for three energy configurations $(E_1, E_2) = (0.1, 0.9)$, $(0.5, 0.5)$, and $(0.9, 0.1)$. The number of particles on each side is 4. The constant C is chosen to be 2.5. We can see that the approximation in equation (3.14) is quite close to the simulation result, especially when x_L is close to 1. Note that we are more interested in the distribution of x_L when it is close to 1, as it is related to the asymptotic dynamics of the full model.

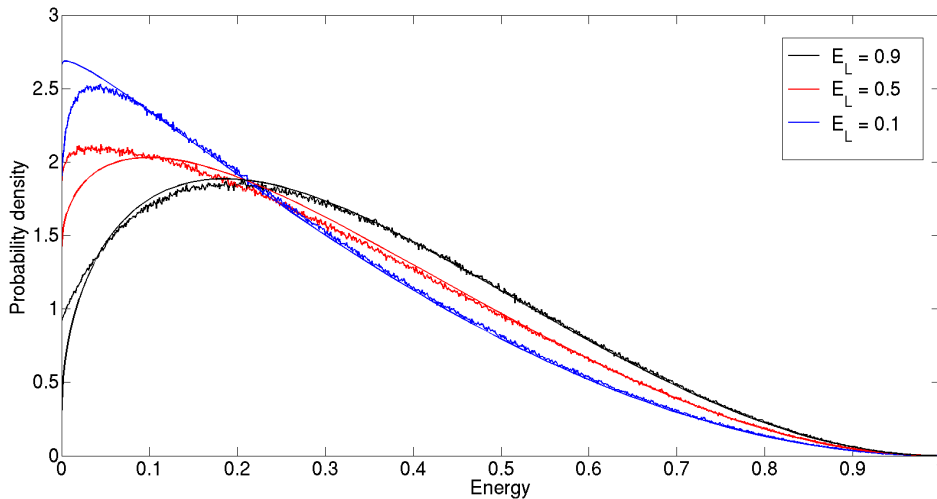


FIGURE 6. Energy distribution of particles participating in a collision.

Therefore, the energy of particles that participate in collision should be $E_1 B_1$ and $E_2 B_2$, where B_1 has the probability density function

$$(3.15) \quad \frac{1}{K} \left(1 + C \frac{E_i}{E_{i+1}} \sqrt{x}\right) (1 - x)^{M-2},$$

and B_2 has the probability density function

$$(3.16) \quad \frac{1}{K'} \left(1 + C' \frac{E_{i+1}}{E_i} \sqrt{x}\right) (1 - x)^{M-2},$$

where C, C' are constants and K, K' are normalizers.

To simplify the model, we only intend to capture the tail behavior of random variables B_1 and B_2 . In other words, we would like to simplify the rule of energy exchange while preserving the right scaling when B_1 (or B_2) is close to 1. The correction term in equation (3.14) does not affect the tail. Hence we simplify B_1 and B_2

to two independent random variables satisfying Beta distributions with parameters $(1, M - 1)$. This assumption is adopted throughout the rest of this paper.

The answer to (b) eventually boils down to the following questions. Consider two rigid disks moving and colliding in a “sufficiently chaotic” billiard table. If the initial kinetic energies are E_1 and E_2 but the initial position and direct of motion are both random, what will the energy distribution of each particle be after the first collision? Without loss of generality, we assume the velocities of two particles are

$$(3.17) \quad \mathbf{v}_1 = \sqrt{E_1}(\cos \alpha, \sin \alpha) \quad , \quad \mathbf{v}_2 = \sqrt{E_2}(\cos \beta, \sin \beta) ,$$

respectively. Let the center of mass of two particles at their first collision be \mathbf{x}_1 and \mathbf{x}_2 . Similarly we let

$$(3.18) \quad \mathbf{x}_1 - \mathbf{x}_2 = 2R(\cos \gamma, \sin \gamma) .$$

Assume two disks have equal mass and their mass center is the geometry center. Then it is easy to see that the post-collision velocities \mathbf{v}'_1 and \mathbf{v}'_2 are

$$(3.19) \quad \mathbf{v}'_1 = \mathbf{v}_1 - \frac{(\mathbf{v}_1 - \mathbf{v}_2, \mathbf{x}_1 - \mathbf{x}_2)}{\|\mathbf{x}_1 - \mathbf{x}_2\|^2}(\mathbf{x}_1 - \mathbf{x}_2)$$

and

$$(3.20) \quad \mathbf{v}'_2 = \mathbf{v}_2 - \frac{(\mathbf{v}_2 - \mathbf{v}_1, \mathbf{x}_2 - \mathbf{x}_1)}{\|\mathbf{x}_2 - \mathbf{x}_1\|^2}(\mathbf{x}_2 - \mathbf{x}_1) ,$$

respectively. Since the total energy is conservative, it is sufficient to calculate $\|\mathbf{v}'_1\|^2$. Some calculation shows that

$$(3.21) \quad \|\mathbf{v}'_1\|^2 = E_1 \sin^2(\alpha - \gamma) + E_2 \cos^2(\beta - \gamma) .$$

Therefore, we only need to find the joint distribution of $\alpha - \gamma$ and $\beta - \gamma$.

Let $\theta_1 = \alpha - \gamma$ and $\theta_2 = \beta - \gamma$. Since a chaotic billiard system converges to its invariant measure (Liouville measure) quickly, it is natural to assume that θ_1 and θ_2 are uniformly distributed on \mathbb{S}^1 . Further we can assume θ_1 and θ_2 to be independent at the collision time, because two billiard systems evolve independently between two collisions. Hence all we need is to find the conditional density of (θ_1, θ_2) when a collision happens. Without loss of generality, we rotate the coordinate such that $\mathbf{x}_1 - \mathbf{x}_2$ is horizontal. Now assume two particles are right before the first collision. It is easy to see that the time to collision is proportional to $(\sqrt{E_1} \cos \theta_1 - \sqrt{E_2} \cos \theta_2)^{-1}$ if $\sqrt{E_1} \cos \theta_1 - \sqrt{E_2} \cos \theta_2 > 0$, and ∞ otherwise. In other words, conditioning on having a collision, the approximate conditional density of (θ_1, θ_2) should be proportional to

$$(3.22) \quad (\sqrt{E_1} \cos \theta_1 - \sqrt{E_2} \cos \theta_2) \mathbf{1}_{\{\sqrt{E_1} \cos \theta_1 - \sqrt{E_2} \cos \theta_2 > 0\}} ,$$

where $\mathbf{1}_A$ is an indicator function with respect to set A .

Therefore, the post-collision kinetic energy of particle 1 equals

$$E_1 \sin^2(\theta_1) + E_2 \cos^2(\theta_2) ,$$

where (θ_1, θ_2) has a joint probability density function

$$(3.23) \quad \frac{1}{L}(\sqrt{E_1} \cos \theta_1 - \sqrt{E_2} \cos \theta_2) \mathbf{1}_{\{\sqrt{E_1} \cos \theta_1 - \sqrt{E_2} \cos \theta_2 > 0\}},$$

and L is a normalizer.

This heuristic argument is justified by our numerical simulation result. In Figure 3.2, we demonstrate the probability density function of the energy of the left particle after a collision, when starting from conditional Liouville measure conditioning on a fixed energy configuration. This matches exactly our analysis about the post-collision energy distribution.

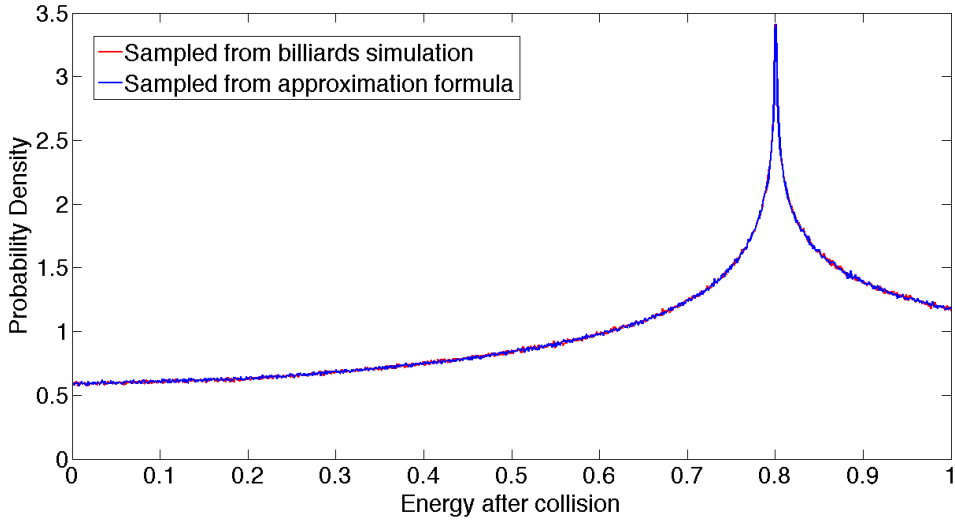


FIGURE 7. Energy distribution after a collision. Two particles with initial energy configuration $(0.8, 0.2)$ and conditional Liouville measure are simulated until their first collision. Red: Probability density function of post-collision energy of the left particle obtained from Monte Carlo simulation with 10^7 samples. Blue: Probability density function of post-collision energy of the left particle given by equation (3.23).

The joint density function in equation (3.23) is too complicated to be interesting. However, it is not hard to see that for each strictly positive energy pair (E_1, E_2) , the distribution of $\|\mathbf{v}'_1\|^2$ has strictly positive probability density everywhere. Same as in (a), we look for a simple expression that preserves the tail dynamics, which is essentially the tail probability that E_1 (or E_2) is very small after an energy exchange. Therefore, for the sake of simplicity, we assume that the energy redistribution is given in a “random halves” fashion, i.e.,

$$(3.24) \quad (E'_1, E'_2) = (p(E_1 + E_2), (1 - p)(E_1 + E_2)),$$

where p is uniformly distributed on $(0, 1)$. This assumption is valid throughout the rest of this paper.

Our numerical simulation shows that this simplification preserves the same tail distribution as well as the same scaling of the energy current. In Figure 8, we show the probability density function of post-collision left cell energy when 3 particles on each side starting with an energy configuration $(E_1, E_2) = (0.5, 0.5)$. One can see a quadratic tail of the probability density function. This means

$$(3.25) \quad \mathbb{P}[E'_1 < \epsilon] \propto \int_0^\epsilon s^2 ds = O(\epsilon^3).$$

Finally, in Figure 9 we plot the average energy flux when each side has 3 particles. The total energy is still set to be 1. We can see that the energy flux is proportional to the difference of cell energy. This further supports the simplified rule of energy exchanges.

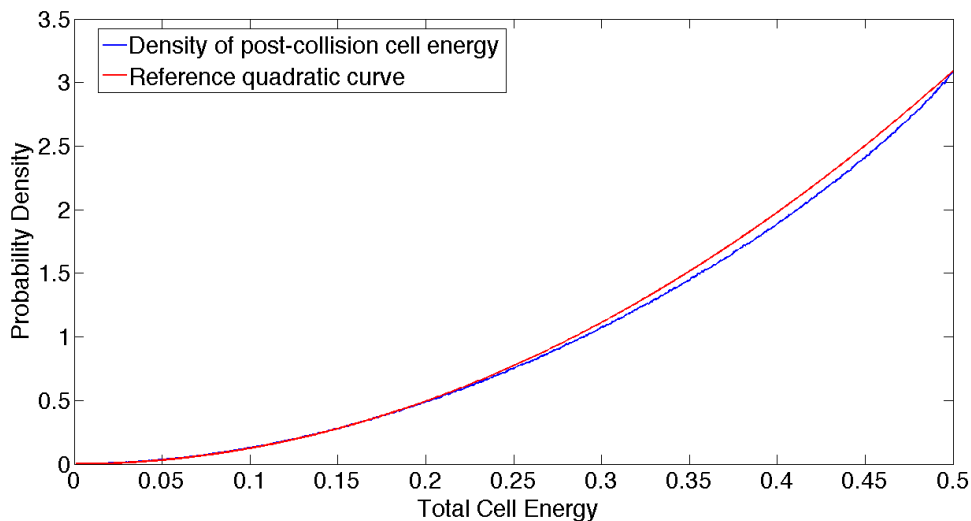


FIGURE 8. Blue: Probability density function of total left cell energy after a collision. Number of particles on each side = 3. Red: A reference quadratic curve. The initial distribution is the conditional Liouville measure conditioning on $(E_1, E_2) = (0.5, 0.5)$. The simple size of the simulation is 10^8 .

In summary, let E_i and E_{i+1} be the total local energy in two neighboring cells, the rule of energy exchange is

$$(3.26) \quad (E'_i, E'_{i+1}) = (E_i - (1-p)E_i B_1 + pE_{i+1} B_2, E_{i+1} - pE_{i+1} B_2 + (1-p)E_i B_1),$$

where B_1 and B_2 are two random variables with Beta distributions with parameters $(1, M-1)$, and p has uniform positive density on $(0, 1)$. Moreover, B_1 , B_2 , and p are independent.

3.3. Stochastic energy exchange model. In summary, the qualitative properties of the nonequilibrium billiard model is preserved by the following *stochastic energy exchange model*.

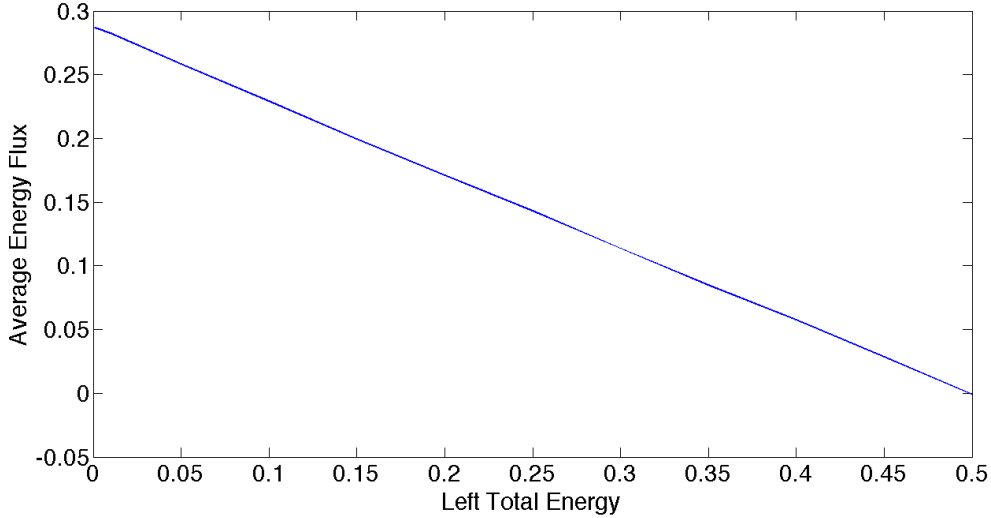


FIGURE 9. Average energy flux from right to left with varying energy configurations. Number of particles on each side = 3. x -axis is the total energy of the left cell E_1 . Initial distributions are conditional Liouville measures conditioning on energy configurations $(0, 1), (0.05, 0.95), \dots, (0.5, 0.5)$. Sample size for each energy configuration is 10^6 .

Consider a chain of N sites that is connected to two heat baths. Let M be an integer that is the model parameter. Each site carries a certain amount of energy. Temperatures of two heat baths are assumed to be T_L and T_R respectively. As discussed in Section 3.1, the energy exchange times can be approximated by a Poisson distribution. Hence an exponential clock is associated to a pair of sites E_i and E_{i+1} . The rate of the clock is $R(E_i, E_{i+1}) = \sqrt{\min\{E_i, E_{i+1}\}}$. When the clock rings, a random proportion of energy is chosen from each site. Then these energies are pooled together and redistributed back randomly. The random proportion satisfies a Beta distribution with parameters $(1, M - 1)$. More precisely, the rule of update immediately after a clock ring is as described in equation (3.26).

The rule of interaction with the heat bath is analogous. Two more exponential clocks are associated to the left and the right heat baths. The rate of the left (resp. right) clock is $R(T_L, E_1)$ (resp. $R(E_N, T_R)$). When the clock ring, the rule of update is

$$(3.27) \quad E'_1 = E_1 - E_1 B_1 + p(E_1 B_1 + X_L B_2),$$

(resp.

$$(3.28) \quad E'_N = E_N - E_N B_1 + p(E_N B_1 + X_R B_2),$$

)

where X_L and X_R are exponential random variables with mean T_L and T_R respectively, p, B_1, B_2 are same as before.

The stochastic energy exchange model generates a Markov jump process \mathbf{E}_t on \mathbb{R}_+^N . We denote P^t by the transition kernel of \mathbf{E}_t . We further define the left operator of P^t acting on a probability measure μ

$$(3.29) \quad \mu P^t(A) = \int_{\mathbb{R}_+^N} \mu(dx) P^t(x, A)$$

and the right operator of P^t acting on a measurable function ξ

$$(3.30) \quad P^t \xi(x) = \int_{\mathbb{R}_+^N} P^t(x, dy) \xi(y).$$

4. COMPARISON OF ERGODICITY OF DETERMINISTIC AND STOCHASTIC MODELS

The reduction from billiard model to the stochastic energy model aims to preserve the long time dynamics. In this section, we will use numerical and analytical tools to verify that asymptotic dynamics are preserved and that the two models have similar ergodicity. For ergodicity, we mean the existence and uniqueness of nonequilibrium steady state, the speed of convergence to steady state, and the rate of correlation decay. Section 4.1 gives a computer assisted proof of ergodicity for the stochastic model. Besides some numerical estimates regarding return times, all arguments are rigorous. In comparison, proving the ergodicity of the nonequilibrium billiard model is much more difficult. Instead, we provide some numerical evidence together with heuristic arguments to justify that the billiard model has the same rate of correlation decay.

4.1. Probability preliminary on ergodicity of Markov processes. A Markov process admits a unique ergodic invariant probability measure under some drift conditions [43, 21]. There are also existing results for the speed of convergence to its invariant measure and the rate of correlation decay [43, 21]. However, these known results can not be applied to the stochastic energy exchange model directly. Even proving the simplest case ($M = 1$) requires advanced techniques and very tedious calculations [39]. It is very difficult to show the speed of convergence through a direct Monte Carlo simulation either. The decay of correlation has small expectation but $O(1)$ variance. To reduce the relative error, a huge amount of samples will be necessary. If the speed of convergence is slow, such a simulation becomes impractical.

Instead, in this subsection we introduce a hybrid approach proposed in [36]. This method circumvents main difficulties of both analytical proof and direct Monte Carlo simulations. It gives an easy and convincing justification of the ergodicity of a Markov process on any measurable state space. Below we will focus on this hybrid method for time continuous Markov processes.

Let Ψ_t be a continuous time Markov process on a measure state space (X, \mathcal{B}) . Let $h > 0$ be a fixed constant. Denote the time- h sample chain of Ψ_t by Ψ_n^h , i.e., $\Psi_n^h = \Psi_{nh}$. Let $\mathcal{P}(x, \cdot)$ be the transition kernel of Ψ_n^h . Further we define $\tau_A(h) = \inf_{t \geq h} \{\Psi_t \in A\}$.

The theory of Markov processes on measurable state spaces is quite different from that of Markov chains on countable spaces. We refer [43] for a detailed review of this

subject. Below we only introduce some necessary terminologies to use the hybrid method in [36].

Let ϕ be a measure on (X, \mathcal{B}) . Ψ_n^h is said to be ϕ -irreducible if for any $x \in X$ and any $A \in \mathcal{B}$ with $\phi(A) > 0$, there exists an integer $n > 0$ such that $\mathcal{P}^n(x, A) > 0$.

A measurable set $\mathfrak{C} \subset X$ is said to be a *uniform reference set* if

$$(4.1) \quad P^h(x, \cdot) \geq \eta\theta(\cdot) \quad \text{for all } x \in \mathfrak{C},$$

where $\theta(\cdot)$ is a nontrivial probability measure.

The Markov chain Ψ_n^h is said to be *strongly aperiodic* if it admits a uniform reference set that satisfies $\theta(\mathfrak{C}) > 0$.

Finally, Ψ_t is said to satisfy the ‘‘continuity at zero’’ condition if for any probability measure μ , we have $\|\mu P^\delta - \mu\|_{TV} \rightarrow 0$ as $\delta \rightarrow 0$, where $\|\cdot\|_{TV}$ is the total variation norm.

By [36], in order to show the polynomial ergodicity of Ψ_t , we need the following four analytical conditions and two numerical conditions.

(A1) Ψ_n^h is irreducible with respect to a non-trivial measure ϕ .

(A2) Ψ_n^h admits a uniform reference set \mathfrak{C} and is strongly aperiodic.

(A3) Ψ_t satisfies the ‘‘continuous at zero’’ condition.

(A4) There exists $\gamma > 0$ such that

$$(4.2) \quad \inf_{x \in \mathfrak{C}} \inf_{t \in [0, h]} P_x[\Psi_t = \Psi_0] > \gamma.$$

(N1) Distributions $\mathbb{P}_\mu[\tau_{\mathfrak{C}}(h) \geq t]$ and $\mathbb{P}_\pi[\tau_{\mathfrak{C}}(h) \geq t]$ have polynomial tails $\sim t^{-\beta}$ for some $\beta > 1$, where π is the numerical invariant measure of Φ_t .

(N2) Function

$$(4.3) \quad \gamma(x) = \sup_{t \geq h} \frac{\mathbb{P}_x[\tau_{\mathfrak{C}}(h) > t]}{t^{-\beta}}$$

is uniformly bounded on \mathfrak{C} .

In [36], we have showed that conditions **(A1) – (A4)**, **(N1)**, and **(N2)** implies the following conclusions.

(a) Ψ_t admits an invariant probability measure π .

(b) Polynomial convergence rate to π :

$$(4.4) \quad \lim_{t \rightarrow \infty} t^{\beta-\epsilon} \|\mu \mathcal{P}^t - \pi\|_{TV} = 0$$

for any $\epsilon > 0$.

(c) Polynomial decay rate of correlation:

$$(4.5) \quad \lim_{t \rightarrow \infty} t^{\beta-\epsilon} C_\mu^{\xi, \eta} = 0$$

for any $\epsilon > 0$ and probability measure μ satisfying **(N1)**, where

$$(4.6) \quad C_\mu^{\xi, \eta}(t) := \left| \int (\mathcal{P}^t \eta)(x) \xi(x) \mu(dx) - \int (\mathcal{P}^t \eta)(x) \mu(dx) \int \xi(x) \mu(dx) \right|.$$

(d) Polynomial convergence rate to π . For any $\epsilon > 0$, we have

$$(4.7) \quad \lim_{t \rightarrow \infty} t^{\beta-\epsilon} \|\delta_x \mathcal{P}^t - \pi\|_{TV} = 0$$

for ϕ -almost every $x \in X$.

(e) Polynomial speed of contraction. For any $\epsilon > 0$, we have

$$(4.8) \quad \lim_{t \rightarrow \infty} t^{\beta-\epsilon} \|\delta_x \mathcal{P}^t - \delta_y P^t\|_{TV} = 0$$

for ϕ -almost every $x, y \in X$.

Note that we did not specify conclusion (e) in [36]. But (e) is a natural corollary of Proposition 4.1 of [36], which implies $\mathbf{E}_x[\tau_{\mathcal{C}}^\beta] < \infty$ for ϕ -almost $x \in X$.

4.2. Verifying analytical conditions. We will first work on the time- h chain \mathbf{E}_n . The verification of condition **(A1)** for \mathbf{E}_n is based on the following Theorem.

Theorem 4.1. *For any set $K \subset \mathbb{R}_+^N$ of the form $K = \{(e_1, \dots, e_N) \mid 0 < c_i \leq e_i \leq C_i, i = 1 \sim N\}$ and any $h > 0$, there exists a constant $\eta > 0$ such that*

$$(4.9) \quad P(\mathbf{E}, \cdot) > \eta U_K(\cdot),$$

for any $\mathbf{E} \in K$, where U_K is the probability measure for the uniform distribution on K .

Proof. This proof is similar to Theorem 5.1 of [36]. We include the proof here for the completeness of the paper. Consider any point $\mathbf{E}^* = \{e_1^*, \dots, e_N^*\} \in K$ and any small vector $d\mathbf{E} = \{(de_1, \dots, de_N), de_i > 0, i = 1 \sim N\}$. Assume $0 < de_i \ll 1$ and let

$$(4.10) \quad B(\mathbf{E}^*, d\mathbf{E}) = \{(x_1, \dots, x_N) \in \mathbb{R}^N \mid e_i^* \leq x_i \leq e_i^* + de_i^*\}$$

be a small hypercube close to \mathbf{E}^* . It then suffices to prove that for any $\mathbf{E}_0 = \{\bar{e}_1, \dots, \bar{e}_N\} \in K$, we have

$$(4.11) \quad P(\mathbf{E}_0, B(\mathbf{E}^*, d\mathbf{E})) > \sigma de_1 de_2 \cdots de_N,$$

where σ is a strictly positive constant that only depends on K .

We then construct the following sequence of events to go from the state \mathbf{E}_0 to $B(\mathbf{E}^*, d\mathbf{E})$ with desired positive probability. Denote the process starting from \mathbf{E}_0 by $\mathbf{E}_t = (e_1(t), \dots, e_N(t))$. Let $\delta = \frac{h}{2N+1}$ and let $\epsilon > 0$ be sufficiently small such that $\epsilon < \min\{c_i, i = 1 \sim N\}$. Let $H = \sum_{i=1}^N (e_i^* + de_i)$. We consider events $A_1 \cdots, A_N$ and B_1, \dots, B_{N+1} , where A_i and B_j specifies what happens on the time interval $(i\delta, (i+1)\delta]$ and $(N\delta + (j-1)\delta, N\delta + j\delta]$, respectively.

- $A_i = \{e_i(i\delta) \in [\epsilon/2, \epsilon]\}$ and $\{\text{The } i\text{-th clock rings exactly once, all other clocks are silent on } ((i-1)\delta, i\delta]\}$.
- $B_1 = \text{Energy emitted by right heat bath} \in (H, 2H)$ and the N -th clock rings exactly once, all other clocks are silent on $(N\delta, (N+1)\delta]$.
- $B_j = \{e_j(N\delta + j\delta) \in [e_{N+2-j}^*, e_{N+2-j}^* + de_j]\}$ and $\{\text{the } (N+1-j)\text{-th clock rings exactly once, all other clocks are silent on } (N\delta + (j-1)\delta, N\delta + j\delta]\}$ for $j = 2, \dots, N+1$.

The idea is that the energy at each site is first transported to the right heat bath, with only an amount of energy between $\epsilon/2$ and ϵ left at each site (events $A_1 \sim A_N$). Then a sufficiently large amount of energy is injected into the chain from the right heat bath (event B_1) so that it is always possible for site j to acquire an amount of energy between e_j^* and $e_j^* + de_j$ by passing the rest to site $j - 1$ (events $B_2 \sim B_{N+1}$), where sites 0 and $N + 1$ denote the left and right heat baths respectively.

It is easy to show that for each parameter M , the probability of occurrence of the sequence of events described above is always strictly positive. Below is a sketch of calculation. We leave detailed calculations to the reader.

- (a) After each energy exchange, the rate of clocks have a uniform lower bound $\epsilon/2$.
- (b) By the rule of energy redistribution, it is easy to see that the probabilities of A_i are strictly positive.
- (c) There is also a uniform upper bound on H given by $2 \sum_{i=1}^N C_i$.
- (d) From the rule of energy redistribution, the probability that $e_j(N\delta + j\delta) \in (e_j^*, e_j^* + de_j)$ after an energy exchange in event B_{j+1} is greater than αde_j for some strictly positive constant α . Hence probabilities of B_j are greater than $\text{const} \cdot de_j$.

In addition, all these probabilities are uniformly bounded from below for all \mathbf{E}^* and \mathbf{E}_0 in K . Hence we have

$$(4.12) \quad \mathbb{P}[A_1 \cdots A_N B_1 \cdots B_{N+1}] \geq \sigma de_1 \cdots de_N$$

for some constant $\sigma > 0$. □

As a corollary, we can prove that \mathbf{E}_n is both strongly aperiodic and irreducible with respect to the Lebesgue measure.

Corollary 4.2. \mathbf{E}_n is a strongly aperiodic Markov chain.

Proof. By theorem 4.1, K is a uniform reference set. In addition $U_K(K) > 0$. The strong aperiodicity follows from its definition. □

Therefore \mathbf{E}_n is strongly aperiodic.

Corollary 4.3. \mathbf{E}_n is λ -irreducible, where λ is the Lebesgue measure on \mathbb{R}_+^N .

Proof. Let $A \subset \mathbb{R}_+^N$ be a set with strictly positive Lebesgue measure. Then there exists a set K that has the form $\{(e_1, \dots, e_N) \mid 0 < c_i \leq e_i \leq C_i, i = 1 \sim N\}$ and $U_K(K \cap A) > 0$.

For any $\mathbf{E}_0 \in \mathbb{R}_+^N$ and the time step $h > 0$, we can choose a $K \subset \mathbb{R}_+^N$ of the form $K = \{(e_1, \dots, e_N) \mid 0 < c_i \leq e_i \leq C_i, i = 1 \sim N\}$ for some $c_i > 0$ and $C_i < \infty$, such that $\mathbf{E}_0 \in K$. Same construction as in Theorem 4.1 implies that $P^h(\mathbf{E}_0, \cdot) > \eta U_K(\cdot)$ for some $\eta > 0$. Therefore, $P^h(\mathbf{E}_0, A) > \eta U_K(A) > 0$. □

Hence assumption **(A1)** and **(A2)** are satisfied.

We can also prove the absolute continuity of π with respect to the Lebesgue measure, which is denoted by λ .

Proposition 4.4. *If π is an invariant measure of \mathbf{E}_t , then π is absolutely continuous with respect to λ with a strictly positive density.*

Proof. This proof is identical to that of Lemma 6.3 of [38]. \square

Condition **(A3)**, or “continuity at zero” follows from the following Proposition.

Proposition 4.5. *For any probability measure μ on \mathbb{R}_+^N , $\lim_{\delta \rightarrow 0} \|\mu P^\delta - \mu\|_{TV} = 0$.*

Proof. This proof is identical to that of Lemma 5.6 of [37]. \square

Condition **(A4)** is trivial as all clock rates are uniformly bounded in any compact set \mathfrak{C} .

4.3. Verifying numerical conditions. Now we are ready to present our numerical results. The demonstrated results are for $N = 3$ and $M = 2$, while our conclusion holds for other parameters we have tested. The uniform reference set \mathfrak{C} is chosen as

$$(4.13) \quad \mathfrak{C} = \{(e_1, \dots, e_N) \mid 0.1 \leq e_i \leq 100, i = 1 \sim N\}.$$

Throughout our numerical justification, we let $h = 0.1$. (Recall that for a time-continuous Markov process Ψ_t , the definition of $\tau_{\mathfrak{C}} = \tau_{\mathfrak{C}}(h)$ depends on h .) Our numerical simulation shows that the tail of $\mathbb{P}_{\mathbf{E}}[\tau_{\mathfrak{C}} > t]$ is $\sim t^{-4}$ for many initial condition \mathbf{E} that we have tested. This is consistent with the heuristic argument. The tail of $\mathbb{P}_{\pi}[\tau_{\mathfrak{C}} > t]$ is a very subtle issue as an explicit formulation of π is not possible. We conjecture that $\mathbb{P}_{\pi}[\tau_{\mathfrak{C}} > t] \sim t^{-3}$.

We have the following argument and numerical evidence to support this conjecture. Consider the simplest case when $N = 1$. If $\pi(\{E_1 < \epsilon\})$ have the tail ϵ^p for all sufficiently small ϵ , then the probability density function at $E_1 = \epsilon$ is $\sim \epsilon^{p-1}$. Since π is invariant, for an infinitesimal $h > 0$, we have

$$(4.14) \quad O(h)\epsilon^M \approx O(h) \int_0^\epsilon s^{p-1} \sqrt{s} ds,$$

where the left term is the probability that $E_1 < \epsilon$ after one energy exchange within $(0, h)$, and the right term is the probability that E_1 exchanges energy with $(0, h)$. This implies $p = M - 1/2$.

One needs to be very careful about the initial distribution when computing the numerical invariant probability measure, as it takes a long time for the model to converge to the steady state. As shown below, the slow convergence mainly occurs at low energy sets. Our strategy is to generate a numerical invariant probability measure from a initial distribution with a correct tail. Let $\mu_0 \sim (\rho_1, \dots, \rho_N)$, where ρ_i is an exponential distribution with mean $(T_L + T_R)/2$. We manually correct the tail of μ_0 before putting it into the Monte Carlo simulation. This manual correction gives a new initial distribution $\mu_1 \sim (\rho_1, \dots, \rho_N)$, where

$$(4.15) \quad \rho_i \sim \begin{cases} \mathcal{E}((T_L + T_R)/2) & \text{if } \mathcal{E}((T_L + T_R)/2) > 0.01 \\ 0.01 u^{(M-1/2)^{-1}} & \text{otherwise} \end{cases},$$

and $\mathcal{E}(\lambda)$ means an exponential random variable with mean λ .

We use the following simulation to justify this correction. The expectation of E_2 versus time is plotted in Figure 10, which is stabilized quickly. In fact, expectations of most observables we have tested converge very fast. However, the slow convergence phenomenon can be captured at the tail, as seen in Figure 11. The tail of $\mu_0 P^{200}$ and $\mu_1 P^{200}$ are compared in Figure 11, in which we find that the low energy tail of μ_0 has not been stabilized yet. This problem is solved by using μ_1 . This prompts us to choose $\hat{\pi} = \mu_1 P^{100}$ as the numerical invariant measure. Our simulation shows that $\mathbb{P}_{\hat{\pi}}[\tau_{\mathfrak{C}} > t] \sim t^{-3}$. (See Figure 12.)

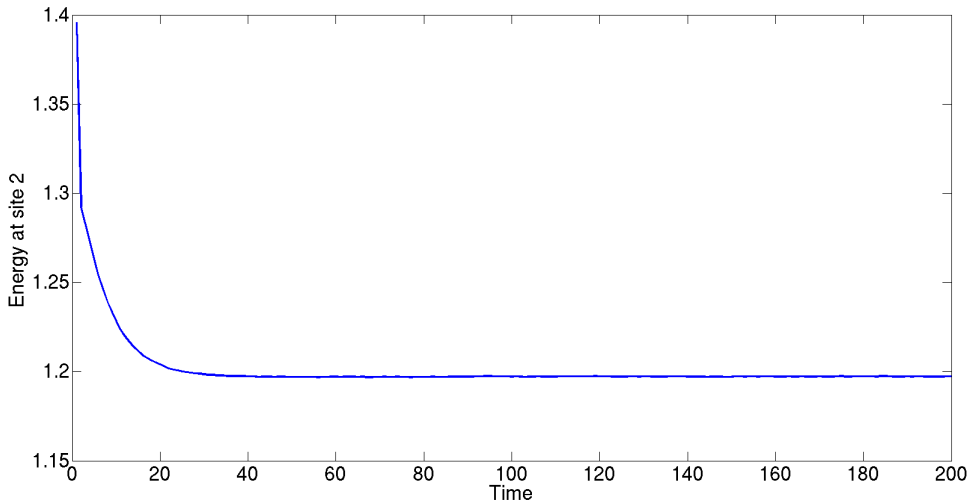


FIGURE 10. Expectation of E_2 vs. time in the stochastic energy exchange model. Model parameters are $T_L = 1, T_R = 2, N = 3$, and $M = 2$. Sample size of Monte Carlo simulation is 10^9 .

It remains to check **(N2)**. We numerically show that

$$(4.16) \quad \gamma(\mathbf{E}) = \sup_{t \geq h} \frac{\mathbb{P}_{\mathbf{E}}[\tau_{\mathfrak{C}} > t]}{t^{-4}}$$

is uniformly bounded on \mathfrak{C} . We follow procedure (a)-(d) in Section 4.1 to show the boundedness of $\gamma(\mathbf{E})$. In fact,

$$(4.17) \quad \gamma_N(\mathbf{E}) = \sup_{1 \leq n \leq N} \sup_{t \geq h} \frac{\mathbb{P}_{\mathbf{E}}[\tau_{\mathfrak{C}} > t]}{t^{-2}}$$

is stabilized very fast with increasing N . We find that a sample of size 10^6 is sufficient for a reliable estimate of $\gamma(\mathbf{E})$. Figure 13 shows that when E_i is small, $\gamma(\mathbf{E})$ decreases monotonically with decreasing E_i for each $i = 1 \sim 3$. Therefore, we expect that the maximal of $\gamma(\mathbf{E})$ in \mathfrak{C} is reached at $\mathbf{E}_* = (0.1, 0.1, 0.1)$. In fact, intuitively one should expect $\gamma(\mathbf{E})$ to decrease with site energy, as starting from low site energy means having higher probability to have even lower site energy after an energy exchange. Finally, we run the simulation again to estimate $\mathbb{P}_{\mathbf{E}^*}[\tau_{\mathfrak{C}} > t]$. As seen in Figure 14, when starting from \mathbf{E}_* , $\mathbb{P}_{\mathbf{E}^*}[\tau_{\mathfrak{C}} > t]$ has a tail $\sim t^{-4}$.

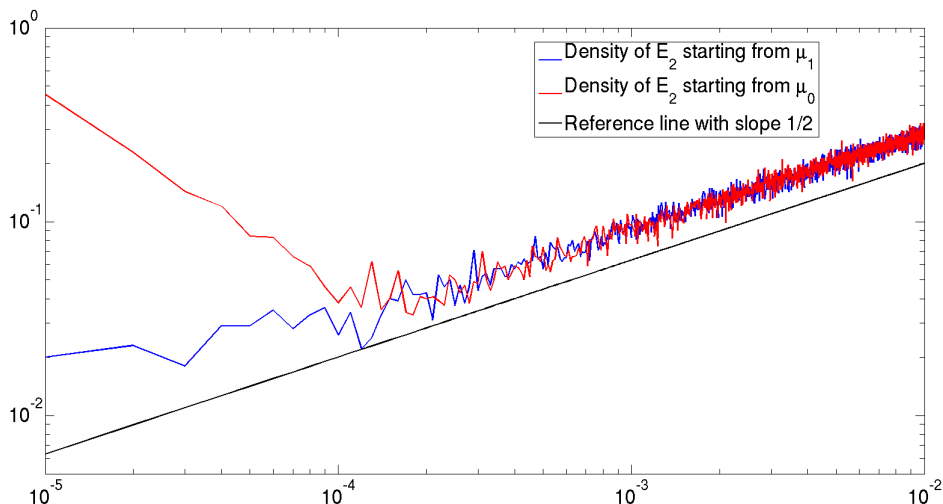


FIGURE 11. Probability density functions of E_2 at $T = 200$ when starting from initial distributions μ_0 and μ_1 in a log-log plot. Model parameters are $T_L = 1, T_R = 2, N = 3$, and $M = 2$. The interval $[0, 0.01]$ are divided into 1000 bins. The probability density is estimated by counting samples whose E_2 falls into each bin at $T = 200$. Sample size of Monte Carlo simulation is 10^9 .

4.4. Main conclusions. The previous subsection verifies two numerical conditions (N1) and (N2) for \mathbf{E}_t with parameter $2M$. The slopes of $\mathbb{P}_{\mathbf{E}^*}[\tau_{\mathcal{E}} > t]$ and $\mathbb{P}_{\pi}[\tau_{\mathcal{E}} > t]$ in the log-log plot are $2M$ and $2M - 1$ respectively.

We also need the uniqueness of π .

Proposition 4.6. *For any $h > 0$, \mathbf{E}_n^h admits at most one invariant probability measure.*

Proof. By the proof of Theorem 4.1, for any $\mathbf{E} \in K$, $P^{h/2}(\mathbf{E}, \cdot)$ has strictly positive density on K . In addition, $P^{h/2}(\mathbf{E}_0, K) > 0$ for any $\mathbf{E}_0 \in \mathbb{R}_+^N$. Hence $P^h(\mathbf{E}_0, \cdot)$ has positive density on K . This implies that every $\mathbf{E}_0 \in \mathbb{R}_+^N$ belongs to the same ergodic component. Therefore, \mathbf{E}_n^h cannot have more than one invariant probability measure. \square

In summary, we have the following conclusions for \mathbf{E}_t . Since now $P_x[\tau_{\mathcal{E}} > t]$ and $P_{\pi}[\tau_{\mathcal{E}} > t]$ have different tails, we can apply conclusions (a) - (e) with $\beta = 2M$ when π is not involved, and $\beta = 2M - 1$ if the initial distribution is π .

- (1) For any T_L, T_R , there exists a unique invariant probability measure π , i.e., the nonequilibrium steady-state, which is absolutely continuous with respect to the Lebesgue measure on \mathbb{R}_+^N .
- (2) For almost every $\mathbf{E}_0 \in \mathbb{R}_+^N$ and any sufficiently small $\epsilon > 0$, we have

$$(4.18) \quad \lim_{t \rightarrow \infty} t^{2M-1-\epsilon} \|\delta_{\mathbf{E}_0} P^t - \pi\|_{TV} = 0.$$

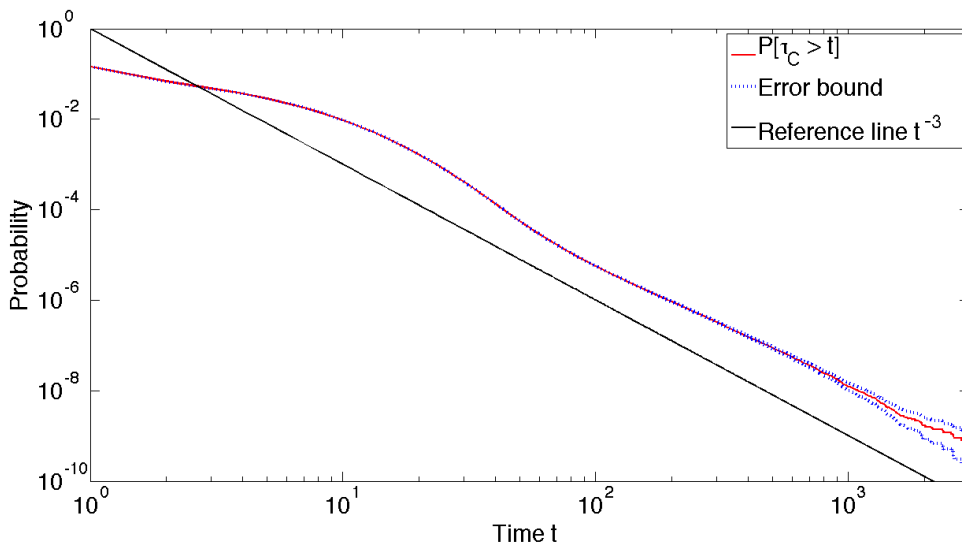


FIGURE 12. $\mathbb{P}[\tau_{\mathcal{C}} > t]$ versus t when starting from $\hat{\pi}$ in a log-log plot. Model parameters are $T_L = 1, T_R = 2, N = 3$, and $M = 2$. Blue dots are the error bar with confidence level 0.95. Black line is a reference line with slope -3 . Sample size of Monte Carlo simulation is 10^{10} .

(3) For any functions $\eta, \xi \in L^\infty(\mathbf{R}_+^N)$, we have correlation decay rate

$$(4.19) \quad C_\mu^{\eta, \xi}(t) \leq O(1) \cdot t^{\epsilon - 2M}$$

for any $\epsilon > 0$ and μ satisfies **(N1)**.

(4) For almost every points $\mathbf{E}_0, \mathbf{E}_1 \in \mathbb{R}_+^N$ and any sufficiently small $\epsilon > 0$, we have

$$(4.20) \quad \lim_{t \rightarrow \infty} t^{2M - \epsilon} \|\delta_{\mathbf{E}_0} P^t - \delta_{\mathbf{E}_1} P^t\|_{TV} = 0.$$

4.5. Ergodicity of the billiard model. The ergodicity of the billiard model is extremely difficult either to prove or to compute. Let Φ_t be the flow of the billiard model, μ be the initial measure, η and ξ be two observables. Theoretically the decay of correlation

$$(4.21) \quad C_{\xi, \eta}^\mu(t) = \left| \int_X \xi(\Phi_t(x)) \eta(x) \mu(dx) - \int_X \xi(\Phi_t(x)) \mu(dx) \int_X \eta(x) \mu(dx) \right|$$

is computable. The speed of decay of correlation gives the ergodicity of the billiard model. However, for large t , $C_{\xi, \eta}^\mu(t)$ has very small expectation and $O(1)$ variance. In order to control the relative error, the sample size of Monte Carlo simulation needs to be very large. In particular, the polynomial tail usually can only be captured for large t . Simple calculation shows that the required sample size can easily exceed the ability of today's computer. See our discussion in [33] for the detail.

Instead, we choose to present the other evidence to support the polynomial speed of correlation decay for the billiard model. The assumption is that when the total

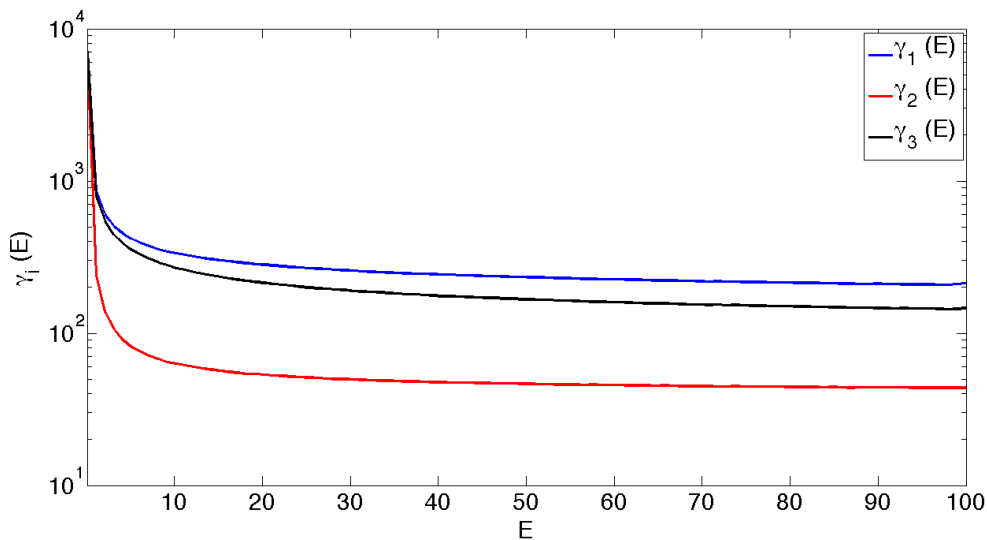


FIGURE 13. The label $\gamma_i(E)$ means replacing the i -th entry of $\gamma(0.1, 0.1, 0.1)$ by E . Model parameters are $T_L = 1, T_R = 2, N = 3$, and $M = 2$. Three curves plot $\gamma_i(E)$ on $[0.1, 100]$ for $i = 1 \sim 3$. Linear-log plot is used because values of $\gamma_i(E)$ changes significantly when E is small.

kinetic energy in both cells are sufficiently high, the decay of correlation is exponentially fast. Therefore, if the first passage time distribution to such a high energy state has a polynomial tail $\sim t^{-\beta}$, we expect the decay rate of correlation to be also $\sim t^{-\beta}$. Although a rigorous justification for this assumption is not possible, this approach can be rigorously proved for simpler deterministic dynamical systems and Markov chains. This is called the “induced chain method”, in which we study the induced Markov chain generated by a set such that the induced chain has exponentially fast mixing. We refer readers to [34] for the induced chain method for Markov processes and [49, 50] for the Young towers for deterministic dynamical systems.

In Figure 4.5, we show the tail distribution of the first passage time to the high energy state

$$(4.22) \quad A = \{(\mathbf{x}_1^1, \mathbf{v}_1^1, \mathbf{x}_2^1, \mathbf{v}_2^1), (\mathbf{x}_1^2, \mathbf{v}_1^2, \mathbf{x}_2^2, \mathbf{v}_2^2) \mid |\mathbf{v}_1^i|^2 + |\mathbf{v}_2^i|^2 \geq 0.2, i = 1, 2\} \subset \Omega$$

for a 2-cell 4-particle model as seen in Figure 2. The total kinetic energy in the system is set to be 1. Since the rate $\sqrt{\min\{E_i, E_{i+1}\}}$ only occurs when one of the total cell energy is sufficiently small (less than 0.01 in our case), we need some importance sampling to reduce the computational cost. The initial cell total cell energy is sampled from the distribution of post-collision total cell energy, conditioning with the event that the left cell energy is less than 0.001. We can see that the tail of first passage time to the high energy set is $\sim t^{-4}$. This supports our claim that the decay rate of correlation should be t^{-2M} if the number of particles in each cell is M .

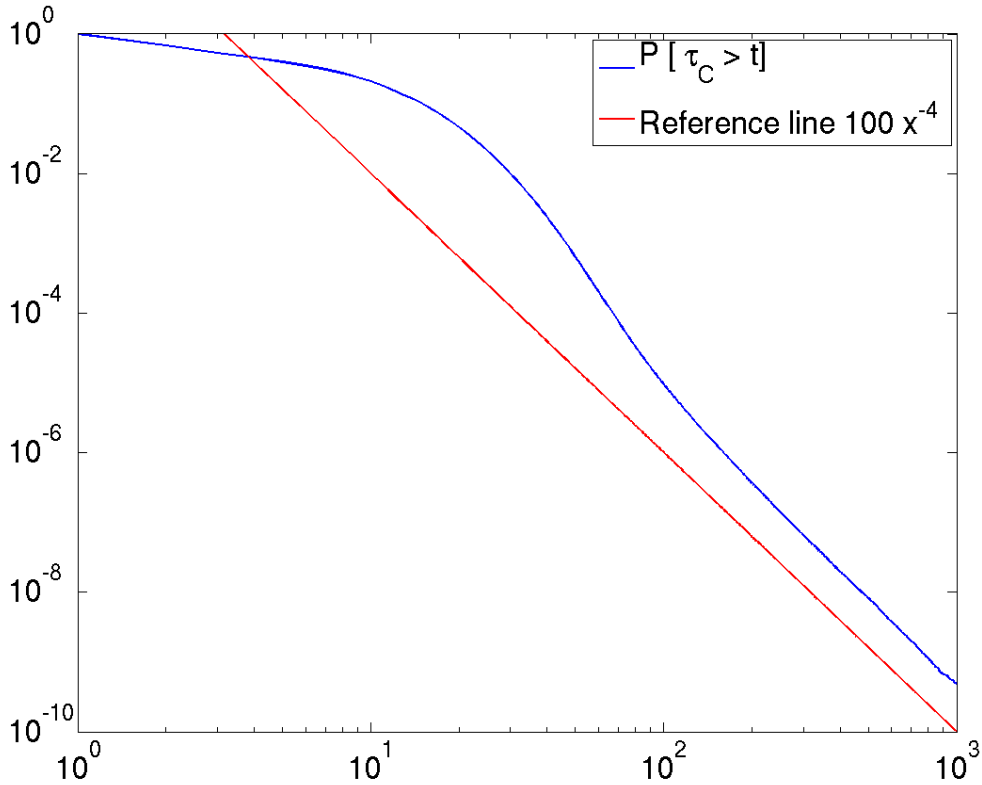


FIGURE 14. $\mathbb{P}_{E^*}[\tau_{\mathcal{C}} > t]$ versus t when starting from E^* in a log-log plot. Red line is a reference line with slope -4 . Model parameters are $T_L = 1, T_R = 2, N = 3$, and $M = 2$. Sample size of Monte Carlo simulation is 10^{10} .

5. COMPARISON OF THERMAL CONDUCTIVITY

It remains to compare the thermal conductivity of the billiard model and that of the stochastic energy exchange model. It has been reported in [16] that the billiard model has a “normal” thermal conductivity, i.e., the thermal conductivity is proportional to the reciprocal of the length of the chain. We use Monte Carlo simulations to verify that the stochastic energy exchange model also has the “normal” thermal conductivity.

We define the empirical thermal conductivity in the following way. Consider a stochastic energy exchange model with N sites and boundary temperatures T_L and T_R respectively. We take the convention that sites 0 and $N + 1$ are the left and the right heat baths respectively. Let $J(t_i, k)$ be the energy flux from right to left if one energy exchange occurs between site k and site $k + 1$ at time t_i . More precisely, we have

$$(5.1) \quad J(t_i, k) = \begin{cases} E'_k - E_k & \text{if } k \neq 0 \\ E_{k+1} - E'_{k+1} & \text{if } k = 0, \end{cases}$$

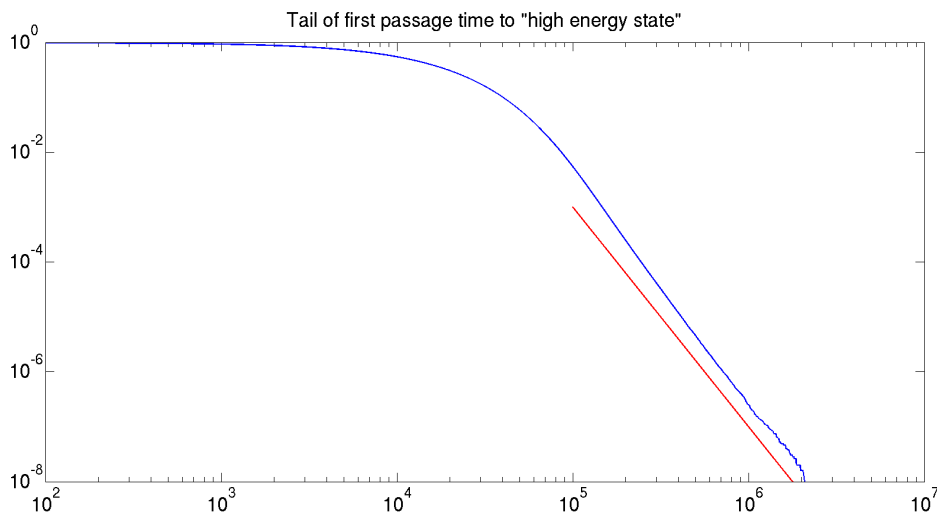


FIGURE 15. Blue: Tail of first passage time $\mathbb{P}[\tau_A > t]$ for the billiard model. Red: reference line with slope -4 . Sample size of the simulation is 10^9 . The initial distribution is a conditional Liouville measure conditioning on the left cell energy is less than 0.001.

if E_k and E_{k+1} exchanges energy at t_i , where E'_k and E'_{k+1} denote the post-exchange energy. When starting from the invariant probability measure π , the *thermal conductivity* is defined as

$$(5.2) \quad \kappa = \lim_{T \rightarrow \infty} \frac{1}{T} \frac{1}{T_R - T_L} \frac{1}{N+1} \sum_{t_i < T} J(t_i, k).$$

In other words, the thermal conductivity measures the average energy flux between each two sites in the chain.

In the numerical simulation, we fix boundary temperatures as $T_L = 1$ and $T_R = 2$. The thermal conductivity is then computed for increasing N . Figure 16 shows the plot of κ vs $1/N$. The least square curve fitting of the plot in Figure 16 gives a linear relation

$$\kappa(N) = \frac{0.0752}{N} + 4.02 \times 10^{-5}.$$

We believe this numerical result confirms that κ is proportional to $1/N$.

6. CONCLUSION

In this paper we study a nonequilibrium billiard model that mimics the dynamics of gas particles in a long and thin tube. Due to the significant difficulty of working on the deterministic interacting particle system directly, we carry out a series of numerical simulations to study the stochastic rule of energy exchanges between cells, which is essentially given by collision events that involves particles from neighboring cells. The time distribution of such events and the post-collision energy distribution are studied. Numerical results show the time evolution of the energy profile of the

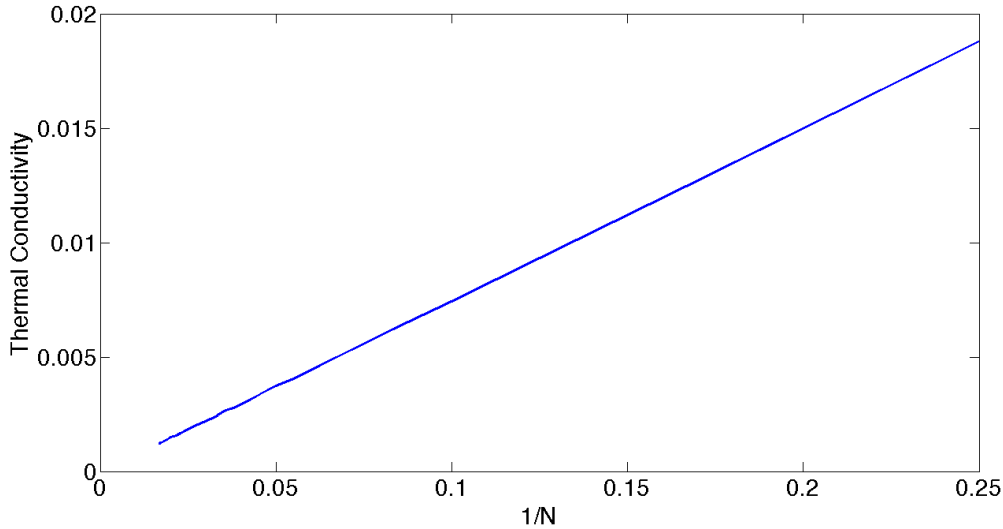


FIGURE 16. Thermal conductivity for the stochastic energy exchange model with $M = 2$. Boundary temperatures are $T_L = 1$ and $T_R = 2$. The length of the chain increases from 4 to 60. The thermal conductivity is computed by averaging 80 results of (5.2) for $T = 60000$.

nonequilibrium billiard model is approximated by a much simpler stochastic energy exchange model. We remark that approximating a difficult chaotic billiard system by a more mathematically tractable stochastic process is a very generic strategy, which can be potentially applied to other highly chaotic billiard-like systems in physics. For example, it is known that Fermi acceleration can be found in many chaotic billiards [29, 30, 31, 41]. And the rate of energy growth is found to be significantly larger in many chaotic billiards or stochastic acceleration models [25, 26].

We then compare the stochastic energy exchange model and the original billiard system. A series of analytical and numerical studies are carried out to study the ergodicity of these models. The conclusion is that the key dynamical properties of the nonequilibrium billiard model is preserved by the stochastic energy exchange model. Both systems have polynomial ergodicity with a speed of correlation decay $O(t^{-2M})$, where M is the number of particles in a cell. In addition, the thermal conductivity of both models is proportional to $1/N$. Simulation algorithms used in this paper are the stochastic simulation algorithm (SSA) [19, 35] and the event-driven billiard simulation algorithm [42] for the stochastic model and the billiard model, respectively.

This result opens the door of many further investigations, as the stochastic energy exchange model is tractable for many rigorous studies. For example, the polynomial ergodicity can be rigorously proved by using the same technique developed in [34]. In addition to the ergodicity, the mesoscopic limit problem is also worth to study. When the number of particles in a cell is large, each collision will only exchange a small amount of energy. Hence the stochastic energy exchange model (after a

time rescaling) has interesting slow-fast dynamics. Such slow-fast dynamics can be approximated by a stochastic differential equation (the mesoscopic limit equation). Many macroscopic thermodynamic properties can be further derived from the mesoscopic limit equation.

This paper serves as the first paper of a sequel that aims to connect billiards-like deterministic dynamics and macroscopic thermodynamic laws. In our forthcoming papers, we will rigorously address the ergodicity, mesoscopic limit, and macroscopic thermodynamic properties of the stochastic energy exchange model derived in this paper.

REFERENCES

- [1] Carlo Boldrighini, Leonid A Bunimovich, and Ya G Sinai, *On the boltzmann equation for the lorentz gas*, Journal of statistical physics **32** (1983), no. 3, 477–501.
- [2] F. Bonetto, J.L. Lebowitz, and L. Rey-Bellet, *Fourier’s law: a challenge to theorists*, Mathematical physics 2000 (2000), 128–150.
- [3] Leonid Bunimovich, Carlangelo Liverani, Alessandro Pellegrinotti, and Yurii Suhov, *Ergodic systems ofn balls in a billiard table*, Communications in mathematical physics **146** (1992), no. 2, 357–396.
- [4] Leonid A Bunimovich, D Burago, N Chernov, EGD Cohen, CP Dettmann, JR Dorfman, S Ferleger, R Hirschl, A Kononenko, JL Lebowitz, et al., *Hard ball systems and the lorentz gas*, vol. 101, Springer Science & Business Media, 2013.
- [5] Leonid A Bunimovich and Ya G Sinai, *Statistical properties of lorentz gas with periodic configuration of scatterers*, Communications in Mathematical Physics **78** (1981), no. 4, 479–497.
- [6] Leonid Abramovich Bunimovich, Yakov Grigor’evich Sinai, and Nikolai Ivanovich Chernov, *Statistical properties of two-dimensional hyperbolic billiards*, Russian Mathematical Surveys **46** (1991), no. 4, 47–106.
- [7] Nikolai Chernov and Roberto Markarian, *Chaotic billiards*, no. 127, American Mathematical Soc., 2006.
- [8] Nikolai Chernov and Lai-Sang Young, *Decay of correlations for lorentz gases and hard balls*, Hard ball systems and the Lorentz gas, Springer, 2000, pp. 89–120.
- [9] Nikolai Chernov and Hong-Kun Zhang, *Billiards with polynomial mixing rates*, Nonlinearity **18** (2005), no. 4, 1527.
- [10] Timothy Chumley, Scott Cook, and Renato Feres, *From billiards to thermodynamics*, Computers & Mathematics with Applications **65** (2013), no. 10, 1596–1613.
- [11] Scott Cook and Renato Feres, *Random billiards with wall temperature and associated markov chains*, Nonlinearity **25** (2012), no. 9, 2503.
- [12] Bernard Derrida, *An exactly soluble non-equilibrium system: the asymmetric simple exclusion process*, Physics Reports **301** (1998), no. 1, 65–83.
- [13] Dmitry Dolgopyat and Péter Nándori, *Nonequilibrium density profiles in lorentz tubes with thermostated boundaries*, Communications on Pure and Applied Mathematics **69** (2016), no. 4, 649–692.
- [14] Jean-Pierre Eckmann, Claude-Alain Pillet, and Luc Rey-Bellet, *Entropy production in non-linear, thermally driven hamiltonian systems*, Journal of statistical physics **95** (1999), no. 1-2, 305–331.
- [15] J.P. Eckmann and L.S. Young, *Nonequilibrium energy profiles for a class of 1-d models*, Communications in mathematical physics **262** (2006), no. 1, 237–267.
- [16] Pierre Gaspard and Thomas Gilbert, *Heat conduction and fourier’s law in a class of many particle dispersing billiards*, New Journal of Physics **10** (2008), no. 10, 103004.
- [17] ———, *Heat conduction and fouriers law by consecutive local mixing and thermalization*, Physical review letters **101** (2008), no. 2, 020601.

- [18] ———, *On the derivation of fourier's law in stochastic energy exchange systems*, Journal of Statistical Mechanics: Theory and Experiment **2008** (2008), no. 11, P11021.
- [19] Daniel T Gillespie, *Exact stochastic simulation of coupled chemical reactions*, The journal of physical chemistry **81** (1977), no. 25, 2340–2361.
- [20] A. Grigo, K. Khanin, and D. Szasz, *Mixing rates of particle systems with energy exchange*, Nonlinearity **25** (2012), no. 8, 2349.
- [21] Martin Hairer, *Convergence of markov processes*, Lecture notes (2010).
- [22] N Haydn, Y Lacroix, S Vaienti, et al., *Hitting and return times in ergodic dynamical systems*, The annals of Probability **33** (2005), no. 5, 2043–2050.
- [23] Nicolai Haydn and Sandro Vaienti, *The compound poisson distribution and return times in dynamical systems*, Probability theory and related fields **144** (2009), no. 3, 517–542.
- [24] SG Jennings, *The mean free path in air*, Journal of Aerosol Science **19** (1988), no. 2, 159–166.
- [25] AK Karlis, PK Papachristou, FK Diakonou, V Constantoudis, and P Schmelcher, *Hyperacceleration in a stochastic fermi-ulam model*, Physical review letters **97** (2006), no. 19, 194102.
- [26] ———, *Fermi acceleration in the randomized driven lorentz gas and the fermi-ulam model*, Physical Review E **76** (2007), no. 1, 016214.
- [27] C. Kipnis, C. Marchioro, and E. Presutti, *Heat flow in an exactly solvable model*, Journal of Statistical Physics **27** (1982), no. 1, 65–74.
- [28] A Krámli, Nandor Simanyi, and Domokos Szasz, *The k-property of three billiard balls*, Annals of Mathematics (1991), 37–72.
- [29] Florian Lenz, Fotis K Diakonou, and Peter Schmelcher, *Tunable fermi acceleration in the driven elliptical billiard*, Physical Review Letters **100** (2008), no. 1, 014103.
- [30] Florian Lenz, Christoph Petri, Fotis K Diakonou, and Peter Schmelcher, *Phase-space composition of driven elliptical billiards and its impact on fermi acceleration*, Physical Review E **82** (2010), no. 1, 016206.
- [31] Edson D Leonel and Leonid A Bunimovich, *Suppressing fermi acceleration in a driven elliptical billiard*, Physical review letters **104** (2010), no. 22, 224101.
- [32] Edson D Leonel, Marcus Vinícius Camillo Galia, Luiz Antonio Barreiro, and Diego FM Oliveira, *Thermodynamics of a time-dependent and dissipative oval billiard: A heat transfer and billiard approach*, Physical Review E **94** (2016), no. 6, 062211.
- [33] Yao Li, *On the stochastic behaviors of locally confined particle systems*, Chaos: An Interdisciplinary Journal of Nonlinear Science **25** (2015), no. 7, 073121.
- [34] ———, *On the polynomial convergence rate to nonequilibrium steady-states*, The Annals of Applied Probability, accepted (2018).
- [35] Yao Li and Lili Hu, *A fast exact simulation method for a class of markov jump processes*, The Journal of chemical physics **143** (2015), no. 18, 184105.
- [36] Yao Li and Hui Xu, *Numerical simulation of polynomial-speed convergence phenomenon*, Journal of Statistical Physics **169** (2017), no. 4, 697–729.
- [37] Yao Li and Lai-Sang Young, *Existence of nonequilibrium steady state for a simple model of heat conduction*, Journal of Statistical Physics **152** (2013), no. 6, 1170–1193.
- [38] ———, *Nonequilibrium steady states for a class of particle systems*, Nonlinearity **27** (2014), no. 3, 607.
- [39] Yao Li, Lai-Sang Young, et al., *Polynomial convergence to equilibrium for a system of interacting particles*, The Annals of Applied Probability **27** (2017), no. 1, 65–90.
- [40] C. Liverani, S. Olla, et al., *Toward the fourier law for a weakly interacting anharmonic crystal*, Journal of the American Mathematical Society **25** (2011), 555–583.
- [41] A Yu Loskutov, AB Ryabov, and LG Akinshin, *Mechanism of fermi acceleration in dispersing billiards with time-dependent boundaries*, Journal of Experimental and Theoretical Physics **89** (1999), no. 5, 966–974.
- [42] Boris D Lubachevsky, *How to simulate billiards and similar systems*, Journal of Computational Physics **94** (1991), no. 2, 255–283.

- [43] Sean P Meyn and Richard L Tweedie, *Markov chains and stochastic stability*, Springer Science & Business Media, 2012.
- [44] Luc Rey-Bellet and L Thomas, *Exponential convergence to non-equilibrium stationary states in classical statistical mechanics*, Communications in mathematical physics **255** (2001), no. 2, 305–329.
- [45] Luc Rey-Bellet and Lawrence E Thomas, *Fluctuations of the entropy production in anharmonic chains*, Annales Henri Poincare, vol. 3, Springer, 2002, pp. 483–502.
- [46] Nándor Simányi, *The k -property of billiard balls I*, Inventiones mathematicae **108** (1992), no. 1, 521–548.
- [47] Nándor Simányi, *Proof of the boltzmann-sinai ergodic hypothesis for typical hard disk systems*, Inventiones Mathematicae **154** (2003), no. 1, 123–178.
- [48] Nándor Simányi and Domokos Szász, *Hard ball systems are completely hyperbolic*, Annals of Mathematics **149** (1999), 35–96.
- [49] Lai-Sang Young, *Statistical properties of dynamical systems with some hyperbolicity*, Annals of Mathematics (1998), 585–650.
- [50] ———, *Recurrence times and rates of mixing*, Israel Journal of Mathematics **110** (1999), no. 1, 153–188.